2014 International Conference on Unmanned Aircraft Systems (ICUAS)
May 27-30, 2014. Orlando, FL, USA

Controller Development and Validation for a Small Quadrotor with Compensation for Model Variation

Chen Wang, Meyer Nahon and Mike Trentini

Abstract— **The research discussed here proposes a control system with compensation to maintain consistent performance for quadrotors under system variations, specifically due to battery drainage and mass changes. This compensation control system is comprised of three subsystems. The first subsystem is a baseline PID controller, which generates a desired rpm for each motor. The second subsystem compensates for battery drainage. Based on a complete relationship of PWM-rpm-Voltage obtained from experiments, this compensation subsystem calculates an appropriate PWM command needed to obtain the rpm received from the PID controller, taking into account the current battery voltage. The last subsystem consists of an online mass estimator to estimate the total mass of the quadrotor and payload, and correspondingly adapts the output of the PID controller in order to maintain performance. Simulation and experiments were conducted, both with and without the compensation strategies. The results clearly show the effectiveness of the proposed approaches.**

I. Introduction

In recent years, small quadrotors have received widespread attention due to their low cost and surveillance capabilities. Proposed applications range from short distance delivery (goods and materials), mapping terrain and finding natural resources, search and rescue, and damage assessment in emergencies (nuclear facilities, earthquake, floods). Some of these missions require quadrotors to fly for a long duration and be capable to pick up or drop off payloads. In these scenarios, system variations due to battery drainage and mass variation can prevent successful mission completion. The control system must be robust enough to ensure consistent vehicle performance in the presence of these system changes.

Many prior works have proposed a variety of control strategies for quadrotors. The PID controller is widely used on quadrotors because of its simple structure. It is also used as a reference for comparison with other control methods [1]-[4]. Backstepping control and sliding mode control are popular nonlinear control strategy [5]-[8]. Neural network and fuzzy control can provide robustness to resist uncertain disturbances such as wind gusts [9]-[12]. Although many control methods have been proposed, few works have considered battery drainage and mass changes that can degrade the performance of quadrotors. Mohammadi and Shahri proposed a Model Reference Adaptive control method to increase the PWM (Pulse Width Modulation) command during battery drainage to maintain desired performance [13]. Min et al. used a robust adaptive controller to tackle unknown payloads and validated it in simulation [14]. Mellinger et al. used least squares method to estimate and compensate for unknown payloads and validated it in both simulation and experiment [15].

The research presented in this paper is based on the Qball-X4, a small commercial quadrotor platform from Quanser Inc shown in Figure 1. We first present a baseline PID controller to control the Qball-X4. This controller provides good performance in both simulation and experiment for short time duration and constant mass.

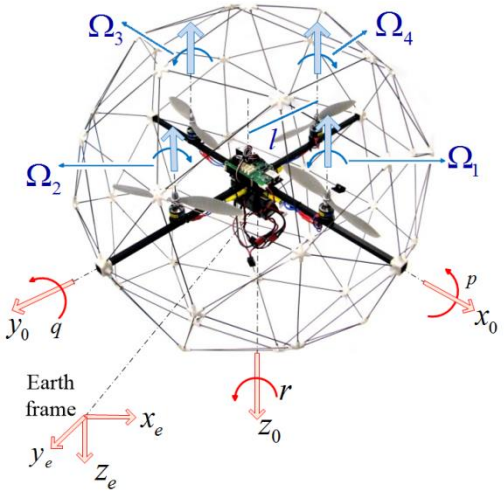

Fig. 1 The Quanser Qball-X4

Most quadrotors are powered by batteries and battery drainage is an unavoidable phenomenon, where the battery voltage drops with time. As a result, the combined performance of the motor-battery also changes, causing the thrust generated by propellers to decrease. This unmodeled effect is difficult for the PID controller to handle. This paper proposes a method to account for the dependency of rpm (revolutions per minute) on PWM (Pulse-width modulation) command and battery voltage. This compensation strategy was evaluated experimentally on the Qball-X4 and was found to be effective.

An autonomous quadrotor should also be able to pick up unknown payloads while accomplishing its mission, without serious performance degradation. Experiments showed that the baseline controller is unable to maintain satisfactory performance during changes of mass, because the control gains cannot sufficiently compensate for the resulting change in the system model. Since, the weight of the payload during a mission may be unknown, an efficient on-line mass estimation subsystem was devised to estimate the total mass of the quadrotor and payload based on information from onboard sensors, and update the controller to generate

C. Wang is with the School of Aeronautics at Northwestern Polytechnical University in Xi'an, China; e-mail: 252430048@qq.com).
M. Nahon is a Professor in the Department of Mechanical Engineering at McGill University, Montreal, Canada (e-mail: meyer.nahon@mcgill.ca).
M. Trentini is with Defence Research and Development Canada, Suffield, Canada (e-mail: Mike.Trentini@drdc-rddc.gc.ca).

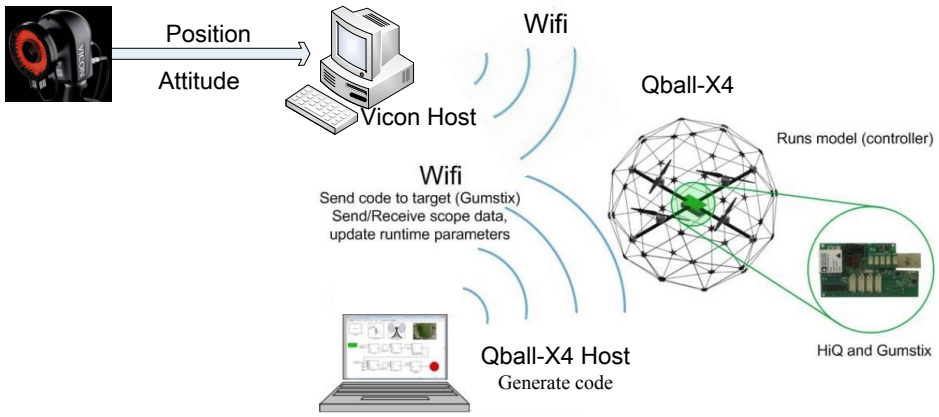

Fig. 2 Structure of the Qball-X4 test platform

sufficient thrust to support the weight. This scheme proved to have fast response to mass variations and showed good performance in simulation and experiments.

II. System Modeling

This section introduces the Qball-X4 platform, and assembles its rigid-body equations of motion

A. System Description

As depicted in Figure 1, Qball-X4 is a small indoor quadrotor, with a mass of 1.5kg. It is surrounded by a carbon fiber cage for safety. It has 2 pairs of propellers, each with a maximum thrust of 5.5 N. Propellers 1 and 3 rotate clockwise (viewed from above), while propellers 2 and 4 rotate counter-clockwise, as shown in Figure 1. Unlike a conventional helicopter which can change the direction of its lift vector by controlling the blade pitch angle, the pitch, roll and yaw of the Qball-X4 are controlled by varying the relative speeds of the four rotors.

The Qball-X4 experimental system includes the following components as shown in Figure 2:

(1) Host computer with Matlab and Simulink. Control system codes can be modified in Simulink on the host desktop and downloaded to the onboard Gumstix microprocessor through a WiFi connection.

(2) Qball-X4. Sensors include an IMU and sonar integrated on the onboard HiQ data acquisition board. The HiQ is able to receive WiFi commands from the host computer and to upload the state of the Qball-X4 (attitude, position, battery voltage) to the host computer, in real time. The controller code is stored in the Gumstix board which operates at 200 Hz frequency. The onboard controller calculates the PWM command for each motor and sends them to 4 ESCs (Electronic Speed Controller) in real time. Each ESC controls a motor/propeller to generate the desired speed.

(3) Vicon motion capture system. The Vicon system measures the vehicle motion by tracking the light reflected from 5 reflective markers fixed on the Qball-X4 frame. The Vicon system determines the position and attitude of the quadrotor and sends these to the HiQ board through WiFi at a rate of 120 Hz.

B. System Dynamics

1) Thrust Model

The thrust T generated by each propeller can be written as:

$$T = k_t \Omega^2 \tag{1}$$

where Ω is the propeller speed and k_t is the thrust coefficient. While generating thrust, the propeller also generates a reaction torque, Q, opposite the direction of rotation of the propeller, which can be written as

$$Q = k_q \Omega^2 \tag{2}$$

where k_q is the reaction torque coefficient.

2) Equations of Motion

Several assumptions are made in order to simplify the airframe equations of motion:

(1) The body of the Qball-X4 is rigid and symmetric.
(2) The four propellers are rigid; no blade flapping occurs.
(3) The vehicle center of mass coincides with the intersection of main frame.
(4) The four propellers work under the same conditions at any time, meaning that k_t and k_q are the same for all propellers.

These assumptions are reasonable because the Qball-X4 operates indoors and at low speed. We define an earth frame and a body frame, and use Euler angles $[\phi, \theta, \psi]^T$ to express the attitude of the quadrotor. The dynamics equations are written in the following form:

$$m\begin{bmatrix}\ddot{x}\\ \ddot{y}\\ \ddot{z}\end{bmatrix} = \begin{bmatrix}0\\ 0\\ -mg\end{bmatrix} + L_{EB}\begin{bmatrix}0\\ 0\\ -U_1\end{bmatrix} + L_{EV}\begin{bmatrix}-\frac{1}{2}C_d\rho V^2 S_{projected}\\ 0\\ 0\end{bmatrix} \tag{3}$$

$$I\begin{bmatrix}\dot{p}\\ \dot{q}\\ \dot{r}\end{bmatrix} = -\begin{bmatrix}p\\ q\\ r\end{bmatrix} \times I\begin{bmatrix}p\\ q\\ r\end{bmatrix} - J_p\begin{bmatrix}q\sum_{i=1}^{4}\Omega_i\\ -p\sum_{i=1}^{4}\Omega_i\\ \sum_{i=1}^{4}\dot{\Omega}_i\end{bmatrix} + \begin{bmatrix}U_2\\ U_3\\ U_4\end{bmatrix} \tag{4}$$

$$L_{EB} = \begin{bmatrix}C_\theta C_\psi & C_\psi S_\theta S_\phi - C_\phi S_\psi & C_\phi C_\psi S_\theta + S_\phi S_\psi\\ C_\theta S_\psi & S_\theta S_\phi S_\psi + C_\phi S_\psi & C_\phi S_\theta S_\psi - C_\psi S_\phi\\ -S_\theta & C_\theta S_\phi & C_\theta C_\psi\end{bmatrix} \tag{5}$$

where $S_{projected}$ is the projected area of the Qball-X4 in the wind direction, C_d is the drag coefficient, and ρ is the air density. In eq. (5), S and C represent the Sine and Cosine function respectively. L_{EB} is a matrix which maps vectors from the body frame to the earth frame, while L_{EV} is a matrix which maps vectors from the wind frame to the earth frame.

In the above equation, $[x, y, z]^T$ represents the position of the vehicle center of mass, expressed in the earth frame, $[p, q, r]^T$ is the angular velocity expressed in the body frame, I is airframe inertia matrix, J_p is moment of inertia of each motor/propeller, $[U_1, U_2, U_3, U_4]^T$ are force and moment inputs generated by propellers. Based on equations (1) and (2), the relationship between $[U_1, U_2, U_3, U_4]^T$ and propeller rotation speeds is as follows:

$$\begin{bmatrix} U_1 \\ U_2 \\ U_3 \\ U_4 \end{bmatrix} = \begin{bmatrix} k_t & k_t & k_t & k_t \\ 0 & -lk_t & 0 & lk_t \\ lk_t & 0 & -lk_t & 0 \\ -k_q & k_q & -k_q & k_q \end{bmatrix} \begin{bmatrix} \Omega_1^2 \\ \Omega_2^2 \\ \Omega_3^2 \\ \Omega_4^2 \end{bmatrix} \tag{6}$$

where l is the distance between center of mass of the vehicle and each motor.

III. Design of the PID Controller

As shown in the preceding section, the Qball-X4 has six degrees of freedom. However, since it has only 4 propellers, it cannot be controlled in all degrees of freedom independently. The four degrees of freedom which can be controlled directly are the three attitude angles and altitude. Control of the $x - y$ position, can be achieved indirectly through control of the pitch (θ) and roll (ϕ). The PID controller is therefore partitioned into an inner loop and an outer loop. The inner loop controls attitude and altitude while the outer loop controls $x - y$ postion.

A. Control Law Synthesis

We define $[x, y, z]^T$ and $[\phi, \theta, \psi]^T$ as the current position and attitude angles respectively. We then define $[x_d, y_d, z_d]^T$ and $[\phi_d, \theta_d, \psi_d]^T$ as the desired positions and attitude angles respectively. The user specifies the desired positions $[x_d, y_d, z_d]^T$ and desired yaw angle ψ_d, while the desired roll and pitch angles are specified by the outer loop controller. Errors components are formed as

$$\begin{bmatrix} \Delta x \\ \Delta y \\ \Delta z \end{bmatrix} = \begin{bmatrix} x_d - x \\ y_d - y \\ z_d - z \end{bmatrix} \tag{7}$$

$$\begin{bmatrix} \Delta \phi \\ \Delta \theta \\ \Delta \psi \end{bmatrix} = \begin{bmatrix} \phi_d - \phi \\ \theta_d - \theta \\ \psi_d - \psi \end{bmatrix} \tag{8}$$

1) Attitude and Altiude Controller

The inner loop PID control laws are:

$$\begin{aligned} F_z &= -\left(\frac{\hat{m}g}{cos\theta cos\phi} - k_z \Delta z_b - k_{dz} \Delta \dot{z_b} - k_{iz} \int \Delta z_b dt\right) \\ T_\phi &= -k_\phi \Delta\phi - k_p p \\ T_\theta &= -k_\theta \Delta\theta - k_q q \\ T_\psi &= -k_\psi \Delta\psi - k_r r \end{aligned} \tag{9}$$

where F_z is the commanded vertical force, while T_ϕ, T_θ and T_ψ are the commanded roll, pitch and yaw moments, resepectively. These are the commanded analogues to $U_1 \rightarrow U_4$. In the vertical force control law, the first term on the right-hand-side of the vertical force equation is intended to support the weight the vehicle, so that this force does not need to be generated by the error terms.

2) Horizontal Position Controller

The outer loop PID control laws are:

$$\begin{aligned} \theta_d &= -k_x \Delta x - k_{ix} \int \Delta x \, dt - k_{dx} \Delta \dot{x} \\ \phi_d &= k_y \Delta y + k_{iy} \int \Delta y \, dt + k_{dy} \Delta \dot{y} \end{aligned} \tag{10}$$

The goal of the outer loop controller is to regulate the pitch and roll angles to obtain the desired vehicle postion in the horizontal plane.

3) Thrust Allocation Algorithm

The thrust allocation algorithm distributes the desired vertical force and moments, specified by eq. (9), among the four thrusters:

$$\begin{aligned} T_1 &= -\frac{F_z}{4} + \frac{T_\theta}{2l} - \frac{T_\psi k_t}{4k_q} \\ T_2 &= -\frac{F_z}{4} - \frac{T_\phi}{2l} + \frac{T_\psi k_t}{4k_q} \\ T_3 &= -\frac{F_z}{4} - \frac{T_\theta}{2l} - \frac{T_\psi k_t}{4k_q} \\ T_4 &= -\frac{F_z}{4} + \frac{T_\phi}{2l} + \frac{T_\psi k_t}{4k_q} \end{aligned} \tag{11}$$

where T_i is the thrust of ith propeller.

4) Calculation of the Propeller Rotational Speeds

Based on the thrust required by the thrust allocation algorithm, we calculate a corresponding propeller rpm using:

$$\Omega_i = \sqrt{\frac{T_i}{k_t}} \tag{12}$$

The PID subsystem, consisting of eqs. (7)-(12), proved to work well in the absence of battery drainage and mass variation, as will be shown in Section III.C

B. Generating the PWM Commands

As noted in Section II, the motors on the Qball-X4 are driven by Pulse Width Modulation (PWM) commands. It is therefore necessary to convert the rpm obtained from eq. (12) into a PWM signal. In the baseline controller, this was done using Figure 3. This figure shows the results of a bench test in which PWM commands were sent to the motor while recording the motor rpm using an optical sensor.

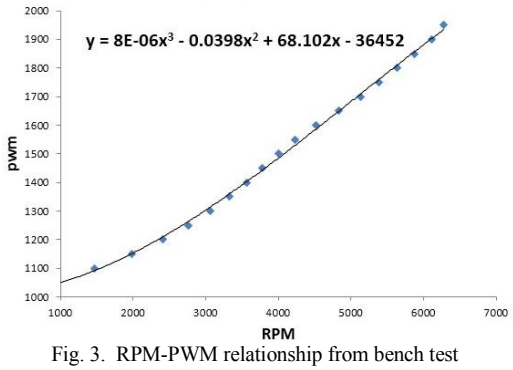

Fig. 3. RPM-PWM relationship from bench test

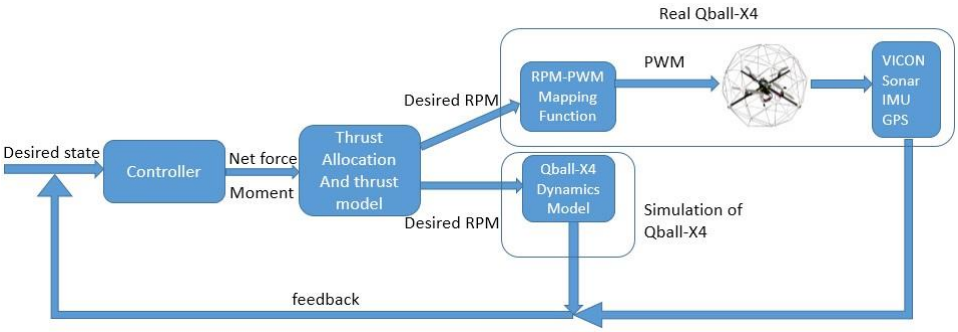

Fig. 4 Baseline PID controller used in experiments and simulation

C. *Simulation and Experimental Validation*

The structure of the baseline Qball-X4 control system is shown in Figure 4. The same controller and control gains (shown in Table I) were applied both in simulations and experiments.

TABLE I CONTROL GAINS

	Proportional	**Integral**	**Derivative**
X	0.12 radm^{-1}	0.12 rad(ms)$^{-1}$	0.01 radm^{-1}s
Y	0.12 radm^{-1}	0.12 rad(ms)$^{-1}$	0.01 radm^{-1}s
Z	1.2 Nm^{-1}	2.8 N(ms)$^{-1}$	0.02 Nm^{-1}s
ϕ	10 Nm(rad)$^{-1}$	--	2 Nms(rad)$^{-1}$
θ	10 Nm(rad)$^{-1}$	--	2 Nms(rad)$^{-1}$
ψ	0.015 Nm(rad)$^{-1}$	--	0.015 Nms(rad)$^{-1}$

A number of simple maneuvers were evaluated to verify proper functioning of the baseline controller.

1) *Takeoff and Hover at 1 m*

The Qball-X4 was commanded to take off and then maintain a hover at 1 meter altitude in both simulation and experiment. Variations of height, propeller speed, PWM command and attitude angles with time are shown in Figure 5. These results shows that PID controller achieves good performance in both simulation and experiment, and that there is a good correspondence between the simulation and the real vehicle.

Figure 5 shows that, for a short duration experiment, the baseline PID controller is able to control the height of the Qball-X4. However, in longer duration experiments, the performance of the height controller deteriorated, as shown in Figure 6. This will investigated in more detail in Section IV.

2) *Step Change of Yaw Angle*

The response of the Qball-X4 to a step change of desired yaw angle from 20 to 0 degree is shown in Figure 7. One pair of propeller increases rpm while the other pair decreases rpm simultaneously by the same amount to generate desired moment T_ψ. Again, the simulation shows good correspondence to the experiment, though there is some oscillation in the experimental steady-state response that is not present in simulation.

3) *Step Change of x-Position*

The simulated response of the Qball-X4 to a step change in desired x-position from 0 to 1 meter is shown in Figure 8.

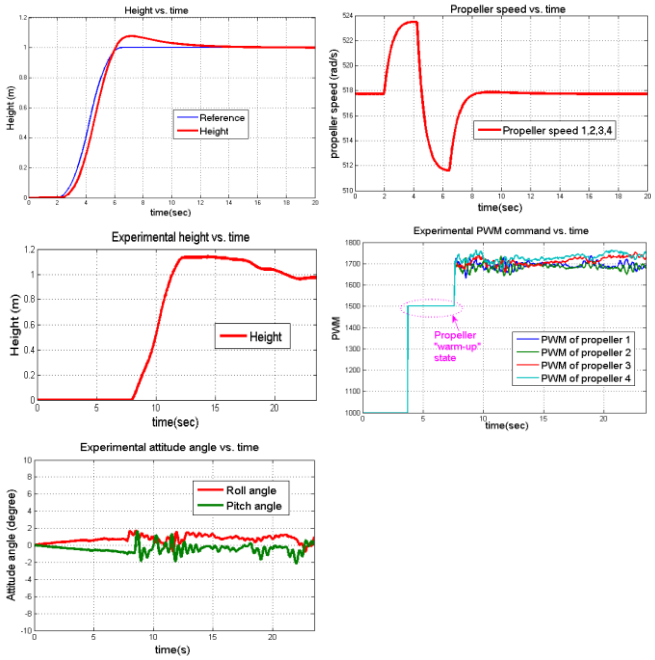

Fig. 5 Takeoff and hover at 1 m

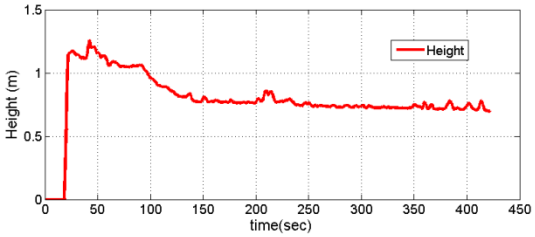

Fig. 6 Height vs. time for long duration experiment

IV. BATTERY DRAINAGE COMPENSATION SUBSYSTEM

The Qball-X4 behavior was found to be quite different with fully-charged batteries and with low battery charge. In particular, it was found that a given PWM command would result in different rpm, depending on battery voltage. The impact of battery drainage caused a particular deterioration in the heave motion, because most of the propeller thrust of a quadrotor is generated to overcome gravity. As shown in Figure 6, the loss of thrust caused by battery drainage could not be overcome by the integral term of the heave controller. An experiment was therefore conducted to better understand the battery drainage phenomenon.

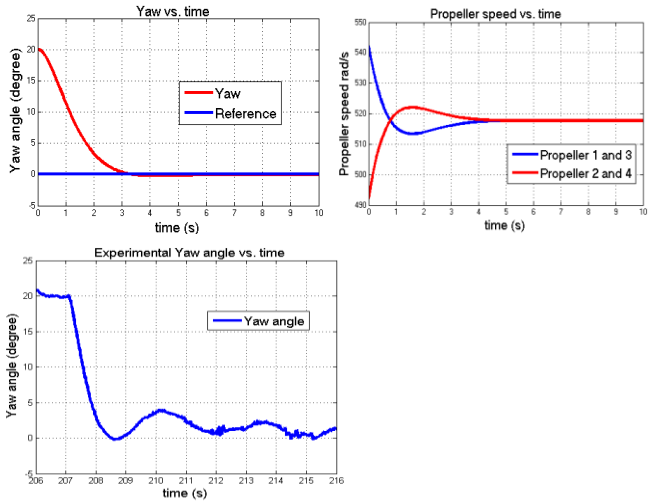

Fig. 7 Step change of yaw angle

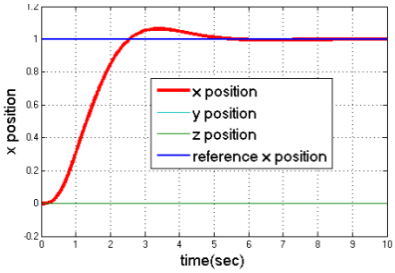

Fig. 8 Step change of x-position

A. *Battery Drainage for a Single Motor*

The Qball-X4 was anchored to the ground, and a constant PWM = 1700µs was sent to one motor. The battery voltage and propeller rpm were recorded by an onboard voltmeter and an optical rpm sensor. The test lasted for 480 seconds. As shown in Figure 9, the rpm dropped from 5200 to 4700 during the test, as the voltage dropped from 12.3 V to 11.1 V. Based on eq. (1), this drop in rpm would result in a 20% loss of thrust.

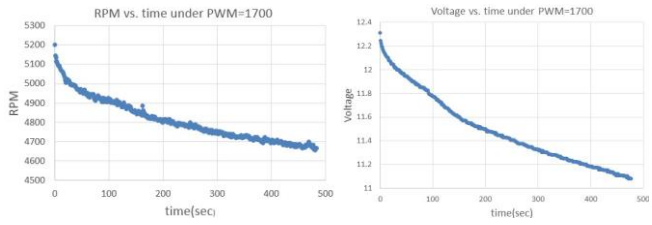

Fig. 9 Battery drainage for a single motor

B. *Complete Relationship of RPM-PWM-Voltage*

Based on these tests, we can conclude that the deterioration of performance evident in Figure 6 is caused by battery drainage which renders the relationship of RPM-PWM of Figure 3, ineffective. A straightforward solution this is to develop a more complete relationship of RPM-PWM-Voltage, that would allow the proper PWM to be calculated, for a given battery voltage, to obtain the desired RPM. This relationship was determined using the following steps:

(1) The motor rpm vs. time and voltage vs. time were recorded for a series of 8 constant PWM commands: 1640, 1670, 1700, 1730, 1760, 1790, 1820, 1850 µs. The result of each experiment was similar to that shown in Figure 9, for PWM = 1700 µs.

(2) The data collected in step 1 was used to generate 8 plots of rpm vs voltage, similar to that shown in Figure 10, for PWM = 1700 µs.

(3) The 8 curves found in step 2 were assembled to create a RPM-PWM-Voltage *surface*, shown in Figure 11.

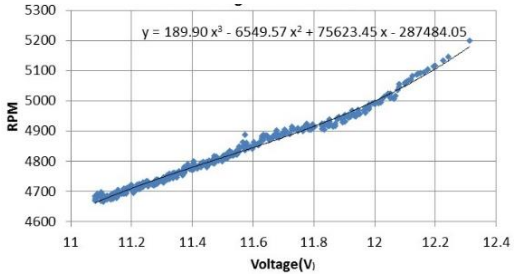

Fig. 10 RPM vs. voltage for PWM=1700 µs

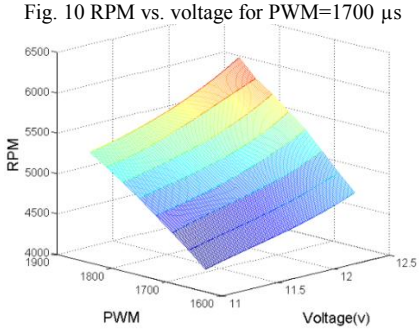

Fig. 11 RPM-PWM-Voltage surface

C. *Battery Compensation Subsystem*

The proposed battery drainage compensation subsystem is shown in Figure 12. This subsystem uses as input a voltage reading from an onboard voltmeter to calculate and appropriate PWM command in real time to obtain the desired rpm generated by the PID controller.

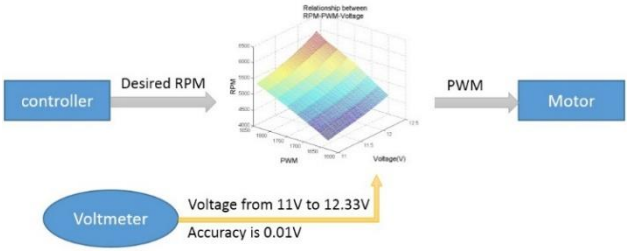

Fig. 12 Battery drainage compensation subsystem

This battery compensation was integrated into the control structure to replace the previous simple RPM-PWM relationship, as shown in Figure 13.

In order to verify this battery compensation strategy, two experiments were conducted. The first experiment was performed on a single motor. A desired command of 5000 rpm was sent to the battery compensation subsystem for about 5 minutes. The commanded PWM, measured voltage and measured rpm were recorded during this test, and the results are shown in Figure 14. While the battery voltage decreased, the commanded PWM was correspondingly

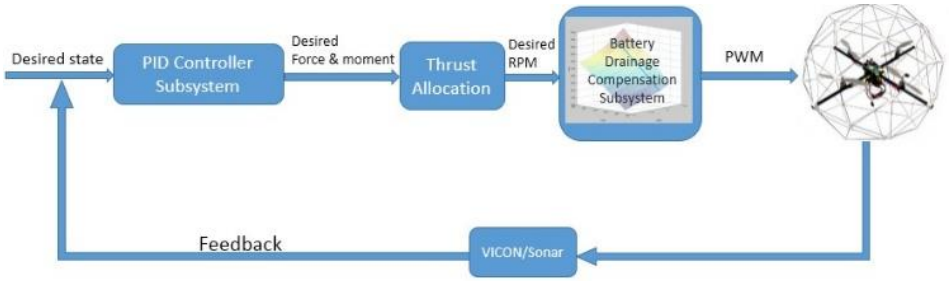

Fig. 13 Control system with battery drainage compensation subsystem

increased by the battery drainage compensation subsystem in order to maintain the desired 5000 rpm. This demonstrated the effectiveness of the proposed compensation scheme.

The second experiment was aimed at testing the battery compensation strategy under real flight conditions. The Qball-X4 was commanded to take off and maintain a hover at 1 m for more than 7 minutes. Figure 15 shows that, during the flight, as the battery voltage dropped, the compensation algorithm increased the PWM commands to maintain thrust. The Qball-X4 successfully maintained a hover at 1 meter. Based on these experiments, it is concluded that the battery compensation strategy can ensure robust system performance during battery drainage.

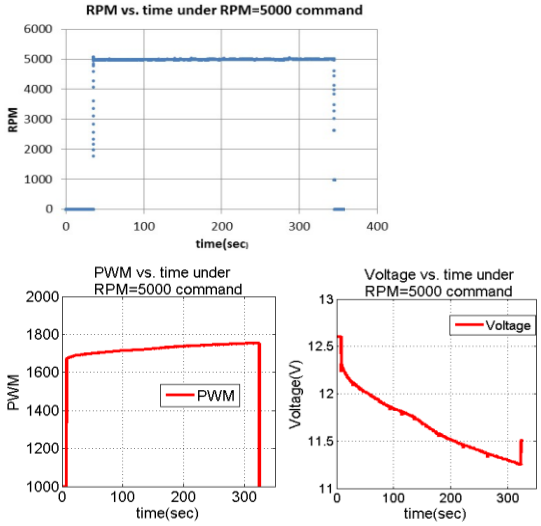

Fig. 14 Ground test for single propeller with battery compensation

V. Mass Compensation Subsystem

As noted earlier, since quadrotor tasks may involve picking up or dropping off payloads of unknown mass, it is important for the controller to be capable of handling this situation. To verify the performance of the baseline PID controller under these circumstances, an experiment with mass variation case was performed. The 1.5 kg Qball-X4 was initially hovering at 1 m. At t = 41 s, a 200g payload was added to the vehicle frame, with the resulting height shown in Figure 16. The PID controller was not able to generate sufficient thrust to compensate for the change in system weight, and, within 3 seconds, dropped to the ground.

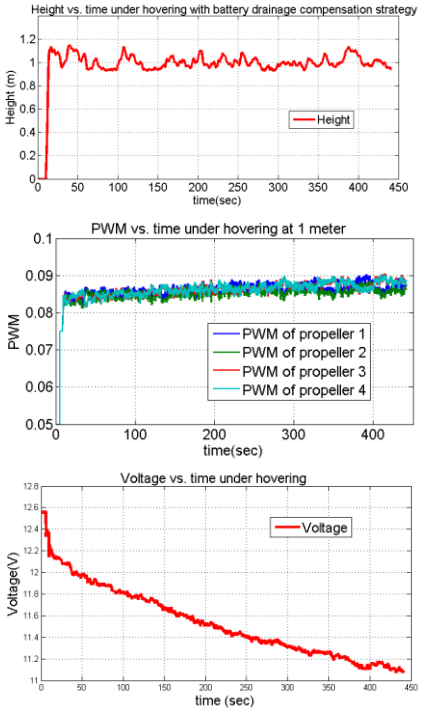

Fig. 15 Flight test of Qball-X4 with battery drainage compensation

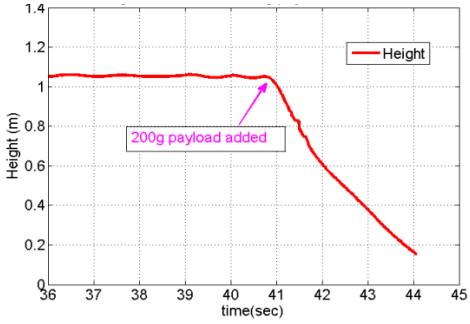

Fig. 16 Height vs. time with 200g payload added at t = 41 s

A. Mass Estimation and Compensation Strategy

In order to address the mass variation problem, a compensation subsystem must be designed to handle payloads of unknown mass. To do this, the scheme must estimate the total mass of quadrotor and payload, and adjust the output of controller automatically. A gradient-based online mass compensation subsystem was devised to estimate the total mass by comparing the commanded vertical force to the measured vertical acceleration. The estimated mass $\hat{m}$ was then used in the vertical PID controller law of eq. (9) to provide compensation.

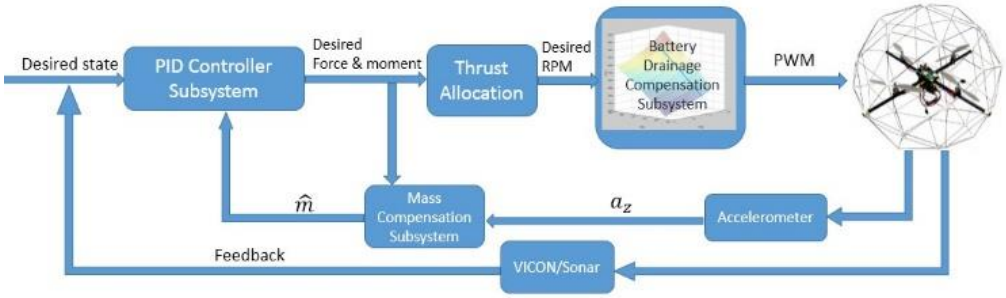

Fig. 17 Complete Control system with model variation compensation

1) Design of Mass Estimator

Since the Qball-X4 normally operates at relatively low pitch and roll angles, the dynamics in the vertical direction can be reasonably simplified to

$$ma_z = mg + F_z \tag{13}$$

where a_z represents the vertical acceleration, and F_z is the desired thrust generated by PID controller. Our goal is to design an estimator to drive $\hat{m}$ to approach the real mass m at a prescribed rate. We first convert eq. (13) into a standard form:

$$(a_z - g) = \frac{1}{m} F_z \tag{14}$$

We then define θ, $\hat{\theta}$ and y as follows

$$\begin{aligned} \theta &= \frac{1}{m} \\ \hat{\theta} &= \frac{1}{\hat{m}} \\ y &= (a_z - g) \end{aligned} \tag{15}$$

Clearly, if $\hat{\theta}$ approaches θ, then $\hat{m}$ will approach m. We can now transfer equations into the standard form of a parameter estimation problem:

$$\begin{aligned} y &= \theta F_z \\ \hat{y} &= \hat{\theta} F_z \end{aligned} \tag{16}$$

To force $\hat{y}$ to approach y, we first define an error term:

$$\varepsilon = y - \hat{y} \tag{17}$$

and we then define an error cost function as:

$$J(\hat{\theta}) = \frac{1}{2}\varepsilon^2 \tag{18}$$

The gradient of $J(\hat{\theta})$ is

$$\nabla J(\hat{\theta}) = -(a_z - g - \hat{\theta} F_z) F_z \tag{19}$$

In order to make the error converge to zero in the quickest way i.e. the steepest descent direction, we choose

$$\begin{aligned} d\hat{\theta}/dt &= -\gamma \nabla J(\hat{\theta}) = \gamma \left(a_z - g - \hat{\theta} F_z\right) F_z \\ \hat{\theta}(0) &= \hat{\theta}_0 = \frac{1}{\hat{m}_0} \end{aligned} \tag{20}$$

where the parameter γ can be adjusted to control the convergence speed. Finally, $\hat{m}$ is calculated from

$$\hat{m} = \frac{1}{\theta(0) + \int d\hat{\theta}} \tag{21}$$

2) Adaptation of PID Controller

Since the baseline heave PID controller already explicitly includes the system mass (see eq. (9)), it is straightforward to feed the estimated mass $\hat{m}$, estimated in real time, into this controller to adapt the controller to the new system weight.

3) Complete Control System

After integration of battery drainage compensation subsystem and mass compensation subsystem with the baseline PID subsystem, the complete control structure shown in Figure 17 is formed. In order to validate this control system, another experiment was performed with mass variation.

C. Experimental Validation of Mass Compensation

The 1.5 kg Qball-X4 was initially in a stable hover at a height of 1 meter, when a 200g payload was added at t = 46 s. As shown in the upper part of Figure 18, when the payload is added, the Qball-X4 first starts to drop, but the estimated mass quickly converges to about 1.7 kg, within 1 second. The controller output correspondingly increases to support the new weight and the height stops dropping at 0.88 m, within 1 second after the mass was added, and then rises in the next 4 seconds back to the desired 1 m. From this experiment, it is apparent that the mass compensation strategy provides robustness to the proposed control system in the presence of mass variations.

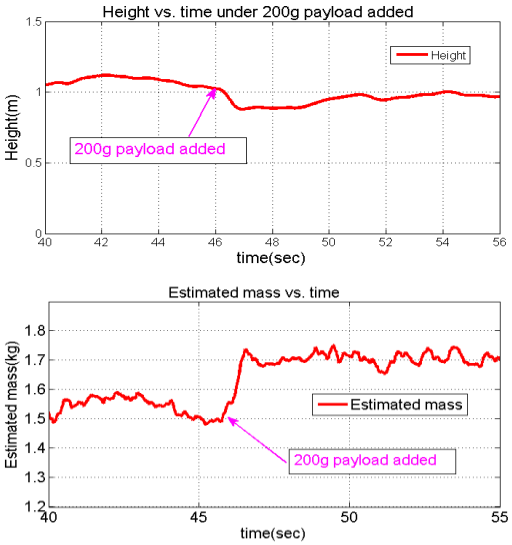

Fig. 18 System response with mass compensation strategy

VI. Conclusion and Future Work

In this paper, a quadrotor controller was presented with compensation strategies to deal with battery drainage and mass variation. Experimental validation of this controller showed that it is effective at dealing with these important effects that would otherwise substantially degrade the system performance. With this control system, the Qball-X4 can fly with consistent performance for a long time duration and safely pick up or drop unknown payloads. Future work will focus on the impact and alleviation of wind gust, which is important for outdoor quadrotors to accomplish missions efficiently and safely.

References

[1] Bouabdallah, S., Noth, A. , and Siegwart, R., "PID vs LQ control techniques applied to an indoor micro quadrotor", IEEE/RSJ International Conference on Intelligent Robots and Systems, Japan, vol.3, pp 2451-2456, September 28 – October 2 2004

[2] Jun Li , and Yuntang Li, "Dynamic analysis and PID control for a quadrotor", 2011 International Conference on Mechatronics and Automation, China, pp 573-578, August 7 to 10 2011

[3] Salih, A.L., Moghavvemi, M., Mohamed, H.A.F. and Gaeid, K.S., "Modelling and PID controller design for a quadrotor unmanned air vehicle", 2010 IEEE International Conference on Automation Quality and Testing Robotics, Romania, pp 1-5, 28-30 May 2010

[4] González-Vázquez, S. and Moreno-Valenzuela, J. "A New Nonlinear PI/PID Controller for Quadrotor Posture Regulation", Mexico, pp 642-647, Sept. 28 2010-Oct. 1 2010

[5] M. Bouchoucha, S. Seghour and H. Osmani, "Integral Backstepping for Attitude Tracking of a Quadrotor System", Electronics and Electrical Engineering, Vol. 116, pp. 75-80, 2011

[6] Das, A., Lewis, F., Subbaro, K. "Backstepping ap¬proach for controlling a quadrotor using lagrange form dynamics". J. Intell. Robot, Syst. Vol. 56, pp. 127–151, 2009.

[7] Ashfaq Ahmad Mian, and Wang Daobo, "Modeling and Backstepping-based Nonlinear Control Strategy for a 6 DOF Quadrotor Helicopter", Chinese Journal of Aeronautics, Vol. 21, pp. 261-268, 2008

[8] T. Madani and A. Benallegue, "Backstepping Sliding Mode Control Applied to a Miniature Quadrotor Flying Robot", 32nd Annual Conference on IEEE Industrial Electronics, France, pp. 700-705, 6-10 Nov. 2006

[9] Nicol, C., Calgary, AB, Macnab, C.J.B., Ramirez-Serrano, A., "Robust neural network control of a quadrotor helicopter", Canadian Conference on Electrical and Computer Engineering, Canada, pp. 1233-1238, 4-7 May 2008

[10] Rabhi, A., Chadli, M., and Pegard, C. "Robust fuzzy control for stabi-lization of a quadrotor", 15th International Conference on Advanced Robotics (ICAR), Estonia, pp. 471- 475, 20-23 June 2011

[11] Fatan, M., Sefidgari, B.L., Barenji, A.V., "An adaptive neuro PID for controlling the altitude of quadcopter robot", 32nd Annual Conference on IEEE Industrial Electronics, Poland, pp. 662-665, 26-29 Aug. 2013

[12] C. Coza, C. Nicol, C.J.B. Macnab, and A. Ramirez-Serrano, "Adaptive fuzzy control for a quadrotor helicopter robust to wind buffeting", Journal of Intelligent & Fuzzy Systems, Vol. 22, pp. 267–283, 2011

[13] Mostafa Mohammadi, and Alireza Mohammad Shahri, "Adaptive Nonlinear Stabilization Control for a Quadrotor UAV: Theory, Simulation and Experimentation", J. Intell. Robot, Syst. Vol. 72, pp. 105-122, 2013.

[14] Byung-Cheol Min, Ji-Hyeon Hong, and Eric T. Matson, "Adaptive Robust Control (ARC) for an Altitude Control of a Quadrotor Type UAV Carrying an Unknown Payloads", 11th International Conference on Control, Automation and Systems, Korea. Oct. 26-29, 2011

[15] Daniel Mellinger, Quentin Lindsey, Michael Shomin and Vijay Kumar. "Design, Modeling, Estimation and Control for Aerial Grasping and Manipulation", 2011 IEEE/RSJ International Conference on Intelligent Robots and Systems, USA, pp 2668 – 2673, September 25-30, 2011